Xu, Z, Bashir, M, Yang, Y, Wang, X, Wang, J, Ekere, NN and Li, C

Multisensory collaborative damage diagnosis of a 10MW floating offshore wind turbine tendons using multi-scale convolutional neural network with attention mechanism

Multisensory Collaborative Damage Diagnosis of a 10MW Floating Offshore Wind Turbine Tendons using Multi-Scale Convolutional Neural Network with Attention Mechanism

Zifei Xu [a,b] , Musa Bashir [a], Yang Yang [c], Xinyu Wang [b], Jin Wang [a] Nduka Ekere[a], Chun Li [b]

a. Liverpool Logistics, Offshore and Marine (LOOM) Research Institute, School of Engineering, Liverpool John Moores University, Liverpool, Byrom Street, L3 3AF, UK

b. School of Energy and Power Engineering, University of Shanghai for Science and Technology, Shanghai 200093，P. R. China

c. Faculty of Maritime and Transportation, Ningbo University, Ningbo, 315211, PR China

Abstract:

An effective damage diagnosis and prognostic management method can considerably reduce operation and maintenance costs of floating wind turbines. In this research, an intelligent damage diagnosis framework, named “MS-ACNN”, has been developed using a multi-scale deep convolution neural network model fused with an attention mechanism. The framework is used to detect, localize, and quantify existing and potential damages on multibody floating wind turbine tendons. The MS-ACNN framework is fitted with two multi-scale extractors, designed to capture multi-scale information from raw wind turbine response signals measured using multi-sensor. The attention mechanism uses weight ratios of extracted damage feature to enhance the MS-ACNN’s capability in offering a better generalization in damage diagnosis. The framework’s performance is examined under normal and noisy environments and with a diagnosis accuracy of 80%, which is higher than those obtained using most generic industrial grade diagnostic tools (MS-CNN-I, MSCNN-II, CNN, CNN-LSTM and CNN-BiLSTM) by at least 10%. The framework is also fitted with a Majority Weighted Voting rule to reduce false alarms and ensure optimum performance of the multi-sensor during collaborative diagnosis.

Further examination shows that the inclusion of a voting rule increases the diagnostic performance's F1 index from 90% and 84% for single- and multi-sensor results to 94%.

Keyword: FOWT, deep learning, structural health monitoring, damage diagnosis, multisensory, maintenance

1. Introduction

Large-scale Floating Offshore Wind Turbines (FOWTs) are increasingly becoming the platforms of choice in offshore clean power generation in order to meet the global target for net zero emission. Future concepts of FOWTs are expected to be of multi-body types, consisting of upper (platform base) and lower (stabilization) tanks for better station-keeping and improved performance. These upper and lower platforms need multiple tendons to connect them together for stability, safety, and reliability purposes [1]. Structural health of the tendons is a prerequisite for safe and stable FOWTs operation. Consequently, intelligent damage diagnosis of tendons including damage localization and quantification is crucial to reducing the maintenance costs [2], [3], [4]. For example, lack of early damage diagnosis of tendons in the first-generation tension leg (TLP) platform has been responsible for tendons' failure and total collapse of the platform [5], [6], [7]. Although modern tension leg platforms are fitted with different kinds of diagnostic tools, recent experience and practice show that these tools cannot be effectively used to diagnose the tendons of FOWTs due to fundamental differences in their operating principles. For example, a 10MW FOWT has a concentrated mass of the nacelle on a slender tower and a wind turbine rotor that is highly sensitive to wind loads, leading to completely different dynamic responses from wind-wave coupling loads to TLP [8]. For such types of structures, the failure probability of FOWT tendons is significantly increased, making it more challenging to achieve optimal safety and reliability for large-scale FOWTs. An effective solution to overcoming these potential challenges requires the development and application of intelligent diagnosis tools, as part of a prognostic and health management (PHM) framework for predictive maintenance. An intelligent diagnosis is a precursor to developing a real-time structural health and operation monitoring and offers the most viable solution to unlocking the huge market potentials of deep-water offshore wind turbines. PHM makes it possible to adopt an appropriate maintenance mode for fundamental components of FOWT structures based on its operating condition (condition-based maintenance) [9]. Consequently, developing a robust PHM framework can lead to a reduced downtime for maintenance, thereby significantly improving operational reliability and reducing maintenance costs [10].

Damage detection, being the first step in PHM, has a main goal of achieving early identification of potential structural changes or damage as part of the real-time monitoring of FOWT tendons' state of health. The significance of early damage detection is that degradation of FOWT tendons' structural strength can be timely detected in order to avoid serious faults [11], [12]. This can considerably reduce the costs of maintenance, increase safety and reliability thresholds, and offers immediate benefits in industrial engineering application.

Current damage diagnosis practice involves the conduct of repeated simulations in order to detect damages on a wind turbine. Majority of existing methodologies for damage detection are based on data-driven methods rather than model-based methods. This is because model-based methods depend on the use of precise mathematical models, which largely limits the accuracy of detection due to high requirement for modeling accuracy. Data-driven methods have advantages in extracting knowledge from historical data, which can be used for fault diagnosis without needing a precise mathematical model. These are some of the reasons data-driven methods are becoming more widely used in detecting faults and conducting diagnosis for FOWT components and systems, such as blades, tower, and tendons or the entire FOWT platform. Generally, data-driven techniques have been made possible by advancements in big data technology like the machine learning techniques. Currently, most of machine learning techniques, including Deep Learning (DL), are being investigated for application in detecting damages and conducting a credible fault diagnosis.

Liu *et al* [13] established a neural network (NN) based damage detection model that is trained by FEM-simulated structural damage datasets. Nguyen *et al* [14] adopted a similar approach in their study by using a numerical simulation to calculate a damage dataset of wind turbine support structures. They used a neural-network-based Structural Health Monitoring (SHM) method for training the model using both time domain and frequency domain data. The results indicated that frequency-domain signals when used as training data for training a NN model have better diagnostic performance. Devilis *et al.* [15] used a PHM method developed based on a shallow neural network to study wind turbines' key structural components. The results confirmed that the NN-based PHM model can detect potential damages before their onset, or they developed into a larger visible crack.

The above damage detection methods are classed as machine learning methods developed based on conventional neural network algorithms but not deep neural networks. However, these methods have some inherent limitations in their application to PHM method when it comes to how artificial feature-extractions and the lack of generalization capability in the models are handled. The pre-processing of features and pattern recognition are supreme requirements in feature extraction engineering because they determine the upper limit of pattern recognition performance [16]. DL can achieve feature extraction and state classification at a faster rate than most of the conventional machine learning methods in existence. This makes its application unique in the development of an effective PHM strategy for floating offshore wind turbines operating in locations where access for inspection and maintenance is often very limited and costly. In addition, this offers a break-through in overcoming the limitations of traditional machine learning algorithms in PHM [17].

Therefore, using the DL technology to develop an intelligent FOWT tendons damage detection for PHM is extremely competitive. Choe *et al* [18] combined Long Short-Term Memory (LSTM) and

Gated Recurrent Unit (GRU) networks to establish a FOWT damage monitoring model. The results show that using the DL technique to develop a PHM model offers a better generalization performance than using a shallow learning method. Xiang *et al*. [19] developed an end-to-end wind turbine damage recognition model for SHM by combining the convolutional networks and recurrent neural networks together. The results indicate that using Convolution Neural Network (CNN) to extract features is more effective than artificially extracting the features. Yang *et al.* [20] used a convolutional network to segment the image information of wind turbine structural damage and went on to establish a diagnosis model based on pixelated features rather than raw vibration signals.

DL models are particularly efficient in developing an intelligent diagnosis framework because of their ability to use both limited and raw vibration signals from a sensor. For large structures such as FOWTs, a single sensor cannot optimally meet the demand for monitoring all the key structural components. Consequently, a new method to effectively monitor multibody platform must use multi-sensor. It must equally consider the impact of maintaining the sensory architecture on FOWTs. Thus far, only limited studies on the application of the DL technique to develop diagnosis models based on multisensory approach to design a PHM framework for FOWT monitoring and maintenance have been reported. These studies largely focused on using multi-sensor SHM methods for wind turbine gearbox diagnosis and maintenance [21], [22], [23], [24]. In the studies, DL algorithms were designed for high-frequency vibration signals, which is unsuitable for application in FOWTs due to their dynamic response signals having long response periods. In addition, the influence of feature-fusion on the performance of a PHM method in multi-sensor method has not been considered in their research. This is very critical to having rational decision-making and information fusion methods in order to develop an intelligent diagnosis framework [25].

From the above literatures, it is evident that intelligent diagnosis algorithms require robust feature extraction and pattern recognition capability for successful application in predictive maintenance. This can be achieved by using a combination of the DL algorithm and attention mechanism to develop an intelligent diagnosis for PHM and maintenance of FOWTs. The combination of a DL with an attention mechanism offers better potential for application in FOWT damage detection than other shallow machine learning algorithms. This is because the combined capability, following the incorporation of an attention mechanism, provides solutions to the use of limited data and the possibilities for intelligent feature extraction. Research on multi-sensor collaborative work to achieve a comprehensive FOWT diagnosis and predictive maintenance shows that both the good generalization of the learning model and the rationality of the collaborative strategy jointly determine the reliability and superiority of an intelligent PHM method. Therefore, considering the key influencing factors of the above-mentioned intelligent PHM method for FOWTs, this study has made the following main contributions:

(1) Development of multi-scale modules fused with a CNN model and an attention mechanism, consisting of multiple multi-scale parallel convolution modules of different depths. The module is designed to capture multi-scale information from responses with different degrees of freedom (DOF) in order to automatically realize the multi-scale feature extraction and improve the neural-network-based model's performance.

(2) Establishing the effectiveness of using FOWT's different DOF responses in training the MS-ACNN model and the resulting impact on the accuracy of the collaborative multisensory module. This was achieved by using a dataset of FOWT tendons with potential damages by accounting the impacts of fully coupled wind-wave loads on a FOWT.

(3) Incorporation of a majority weighted hard-voting rule, using a Particle Swarm Optimization (PSO) algorithm, to fuse outputs from the MS-ACNN model in the decision-making level to ensure that the performance of multisensory feature fusion can improve the robustness of the intelligent diagnosis method of FOWTs.

2. Modelling Structural Damage on Floating Offshore Wind Turbine Tendons

Details of the FOWT model used in this study and methodology for modelling tendon damages are provided in this section.

2.1. The structural model of the 10MW multi-body Floating Offshore Wind Turbine

In this study, a 10MW multibody TELWIND floating wind turbine structure is used to support the 10MW DTU baseline wind turbine. A model of the 10MW TELWIND platform is presented in Figure 1.

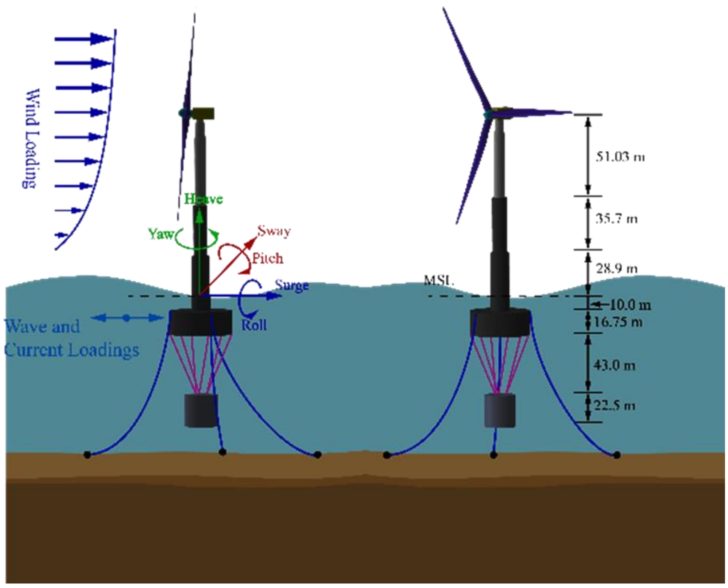

Figure 1: A model of the 10 MW TELWIND wind turbine

The 10 MW TELWIND FOWT is designed for application in 110 m water depth or deeper offshore locations. For station-keeping purposes, the mooring lines configuration has been modified for application in the selected location. The platform consists of an upper tank (UT) and a lower tank (LT). The UT is located at 10 m below mean water level (MWL) and has a 16.75 m draught. The LT's draught is 22.5 m. The platform has a combined total draught of 92.25 m. Both UT (diameter of 44.5 m) and LT (diameter of 23 m) have a cylindrical geometry. The length of each tendon is 48.81 m with a diameter of 0.271 m.

2.2 Modelling of damage scenarios

The dynamic response of the 10 MW FOWT structure which consists of a cylindrical platform's base (Upper Tank), a ballast tank (Lower Tank) connected by tendons (6) and the mooring lines for station-keeping are simulated as a coupled system. This is done to obtain the requisite datasets for different tendon damage scenarios needed for the damage diagnosis and PHM.

In order to ensure that the predicted response data accurately represents the dynamics of the prototype TELWIND FOWT, a coupled (FAST and AQWA, F2A) numerical tool is used to conduct the FOWT aero-hydro-servo-elastic analysis. The framework of the coupling tool is presented in Figure 2.

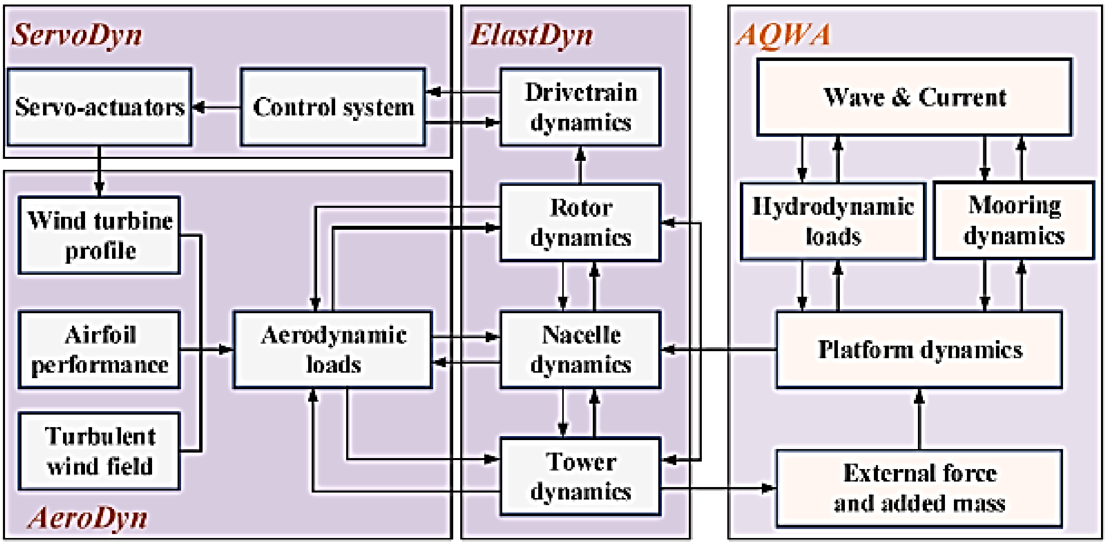

Figure 2: Flowchart of F2A Module

AeroDyn, ElastDyn and ServoDyn modules of FAST are integrated in AQWA using a dynamic link library (DLL) in order to calculate the wind turbine platform's response based on solutions of dynamic equation of motion. The coupled numerical tool is designed to capture the platform's responses in all DOFs. The tool can conduct arbitrary simulation of the damage scenarios in a coupled mode with F2A as described in ref [26]. The significance of the coupled analysis is to ensure that platform responses are included in the real-time prediction of tendons' responses based on cable dynamics using finite element method. Each tendon is discretized into finite lengths with their individual masses applied at the centroid of the unit element as concentrated mass. Figure 3 shows a diagram of the forces acting on a unit tendon length.

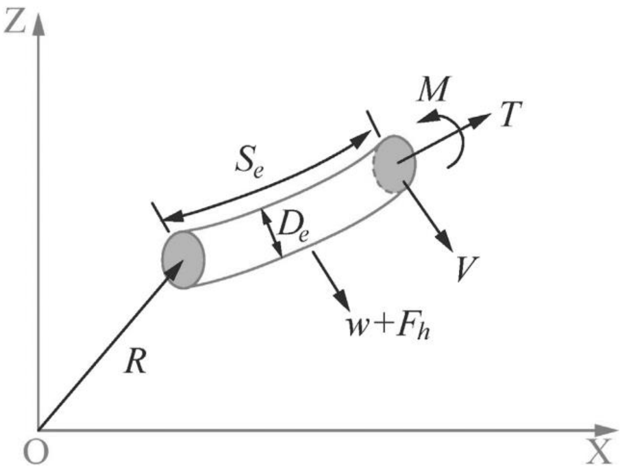

Figure 3: Forces and moment on a discretized tendon element

Dynamic responses of the tendon modelled as a cable element are calculated using Equation 1.

$$\begin{cases} \dfrac{\partial \mathbf{T}}{\partial S} + \dfrac{\partial \mathbf{V}}{\partial S} + \mathbf{w} + \mathbf{F} = m\dfrac{\partial^2 \mathbf{R}}{\partial t^2} \\ \dfrac{\partial \mathbf{M}}{\partial S} + \dfrac{\partial \mathbf{R}}{\partial S} \times \mathbf{V} + \mathbf{q} = \mathbf{0} \end{cases} \tag{1}$$

where **T** and **V** are the tensile force and shear force vectors acting on the node of a unit tendon length, respectively; **R** is the unit tendon length's position vector. **S** denotes the un-stretched length of a unit tendon in an unloaded condition; **w** and **F** are the respective unit weight and hydrodynamic load acting on the tendon element; **M** is the nodal bending moment vector acting on the unit tendon's node; **q** is the unit tendon's distributed moment per length.

The nodal bending moment and tensile force acting on each unit element are calculated using Equation 2.

$$\begin{cases} \mathbf{M} = EI \cdot \dfrac{\partial \mathbf{R}}{\partial S} \times \dfrac{\partial^2 \mathbf{R}}{\partial S^2} \\ \mathbf{T} = EA \cdot \varepsilon \end{cases} \tag{2}$$

where ε is the stretched length; EA and EI are the corresponding nodal axial and bending stiffnesses acting on a unit tendon element. The tendon stiffness is equal to zero in the event of a failure occurring at any specific instant or during the examination of the tendon breakage scenario.

All six tendons have been modelled to have damage magnitudes ranging from 5% to 50% and they are accordingly simulated to develop a potential damage dataset of the tendon structure. The potential damage is defined by changes in the tendon stiffness. The dataset includes six DOF responses of the tendon systems, recorded as displacement, velocity, and acceleration on the upper tanks of the coupled FOWT system. However, only the acceleration dataset was used for the damage diagnosis study. Detailed wind-wave conditions used in the simulations of tendon damages are presented in Table 1. The observed wind-wave conditions data were measured from 2011 to 2016 [27].

Table 1：Details of wind-wave conditions for the FOWT dataset prediction.

Value	Values /(Probabilities)			
Wind direction / (°)	120.6 / (23.6%)	233.1/ (76.4%)		
Wind speed /(m/s)	7.8 / (27.8%)	10.0 / (33.3%)	12.0 / (25.0%)	14.2 / (13.9%)
Significant wave height /(m)	1.8 / (25.0%)	2.4 / (33.3%)	3.6 / (41.7%)	
Spectral peak period /(s)	4.4 / (44.4%)	5.7 / (23.6%)	7.0 / (32.0%)	
Current direction / (°)	96.8 / (51.4%)	275.6 / (48.6%)		
Current speed /(m/s)	0.22 / (100%)			

Simulations of the coupled 10MW platform to predict the tendon damages are conducted based on two wind directions, 120.6° and 233.1° with corresponding probabilities of occurrence of 23.6% and 76.4%. Four wind speeds are selected to generate the unsteady based on Kaimal wind spectrum wind by using NREL TurbSim. For the wave conditions, three main significant wave heights with their corresponding peak periods have been used in the simulations. In addition, the simulation considered a constant current speed by including the effects of current acting in two directions, 96.8° and 275.6° with corresponding probabilities of occurrence of 51.4% and 48.6% respectively. The parameters setting is further described in ref. [1].

3. Principles of the Potential Tendon Damage Detection Methodology

In this study, parallels of 1-D convolutional neural network modules with different network depth, including polling and activation layers, batch normalization and fully connected layer, are used as a multi-scale unit in the module for features extraction. The multi-scale feature extractor module is composed of parallel convolution groups designed to directly extract features from the FOWT response signals without a need for an intervening algorithm. This process eliminates a requirement for manual operation, making the whole algorithm self-adaptive.

3.1 The multi-scale feature-extractor

The newly designed feature extractor unit is composed of convolution, pooling, activation and batch normalization algorithms fused together to provide optimum performance. The mathematical formulas governing the design of the algorithms and their corresponding functions are given as follows.

In the convolution unit, the convolutional process is given by Equation 3, in which $\mathbf{K}_i^l$ is the i^{th} filter in the pooling and activation layers l. $\mathbf{X}^{l(\mathrm{R}^j)}$ is the j^{th} local area in the convolutional layer l.

$$y^{l(i,j)} = \mathbf{K}_i^l \cdot \mathbf{X}^{l(\mathrm{R}^j)} = \sum_{j'=0}^{W} \mathbf{K}_i^l(j')\mathbf{X}^{l(j+j')} \tag{3}$$

where $y^{l(i,j)}$ is the dot product of convolution kernel and the local area. *W* denotes the width of the convolution kernel and $\mathbf{K}_i^l(j')$ represents the j^{th} weight of the convolutional layer's kernel *l*.

In order to enhance the capability of the algorithm to capture and express non-linearity in the input signal and make its learned features more easily identifiable, an activation function, Rectified Linear Unit (ReLU), is integrated into the algorithm and placed immediately after the convolutional layer. A mathematical representation of the ReLU activation function is given by Equation 4:

$$a^{l(i,j)} = f(z^{l(i,j)}) = \max\{0, z^{l(i,j)}\} \tag{4}$$

where $z^{l(i,j)}$ denotes the Batch Normalization (BN) output array and $a^{l(i,j)}$ represents the activation function of $z^{l(i,j)}$.

The BN technique is introduced before the pooling operation to ensure that the network training is efficiently accelerated and potential problems of gradient disappearance, which are typically caused by an activation function, are eliminated. The BN technique includes an n-dimensional array ($\mathbf{y}^{l} = (y^{l(1)}, y^{l(2)}, \ldots, y^{l(n)})$ up to the l^{th} BN layer), represented as $\mathbf{y}^{l(i)} = (y^{l(i,1)}, y^{l(i,2)}, \ldots, y^{l(i,n)})$ and $\mathbf{y}^{l(i)} = y^{l(i)} = y^{l(i,1)}$ when the BN layer is changed from its initial position before the pooling operation unit to a new position just after convolutional and fully connected layers. A general equation for calculating the BN operation is given as follows by Equation 5 and it is a sub-component in Equations 6 - 7:

$$\hat{y}^{l(i,j)} = \frac{y^{l(i,j)} - \mu}{\sqrt{\sigma^2 + \varepsilon_S}}, z^{l(i,j)} = \gamma^{l(i)} \hat{y}^{l(i,j)} + \beta^{l(i)} \tag{5}$$

$$\mu = \frac{1}{n} \sum_{i=1}^{n} y^{l(i,j)} \tag{6}$$

$$\sigma^2 = \frac{1}{n} \sum_{i=1}^{n} (y^{l(i,j)} - \mu)^2 \tag{7}$$

where $z^{l(i,j)}$ is the output of a neuron. μ and σ^2 are respectively the mean and variance of $y^{l(i,j)}$. ε_S is a negligible constant added to stabilize the calculation and prevents it from becoming invalid when the variance is zero. $\gamma^{l(i)}$ and $\beta^{l(i)}$ are the respective scale and shift parameters to be learned from the extracted features.

Another important component of the algorithm is the pooling layer, also referred to as the down-sampling layer. The pooling layer is significant because it provides the algorithm with capability of reducing the dimensional lengths and the number of parameters to be learned in the extracted features within the neural network. The algorithm used in this research adopted the maximum pooling technique instead of the average pooling technique (both of which are commonly available). The mathematical representation of the selected pooling technique is presented in Equation 8.

$$p^{l(i,j)} = \max_{(j-1)W+1 \le t \le jW} {}^{\{a^{l(i,t)}\}} \tag{8}$$

where $a^{l(i,t)}$ denotes the t^{th} neuron value in the i^{th} framework of layer l; the width of the pooling size is represented by W; $p^{l(i,j)}$ is the corresponding value of the neuron in layer l of the pooling unit, and $t \in [(j-1)W+1, jW]$.

Features extracted by the convolution layer have probability distributions from each intrinsic mode function (IMF) that are directly transmitted into the fully connected layer for the purpose of feature classification. The resulting output from the classification is accordingly grouped into a probability entity by the softmax function φ, defined by Equation 9 as:

$$\varphi(u_c) = e^{u_c} \Big/ \sum_{c=1}^{T} e^{u_c}, c = 1, 2, \ldots, T \tag{9}$$

where $\varphi(u_c)$ is a T-dimensional probability vector, which represents the probability distribution under T^{th} test scenario, u_c denotes the extracted output from each one dimension (1-D) CNN.

Following a motivation by Zhao and Jiang's studies [28], [29], this research uses a large convolution kernel because of its good receptive field that can be controlled by the size of the kernel. However, Zhao and Jiang's studies merged the advanced features on the first and last layers, which made it unsuitable for application in FOWTs because of its inherently slow response cycles. Therefore, in the proposed multi-scale feature extractor developed in this research, the depth of the network has also become a factor for the model to control the advancement of multi-scale features. In addition, the model is fitted with an attention mechanism to equip it with capability to evaluate the contributions of the advanced fault or damage features that correspond to each extracted features from the multi-scale feature extractor [30]. The advanced channel features are adaptively weighted by the attention mechanism. The weighted features are fused and fed into the classification layer for the purpose of calculating their respective probabilities.

A schematic representation of the MS-ACNN model with the designed multi-scale feature extractor is presented in Figure 4. The FOWT acceleration responses used for the damage diagnosis are the response signals on the tendons measured based on relative responses of UT and LT.

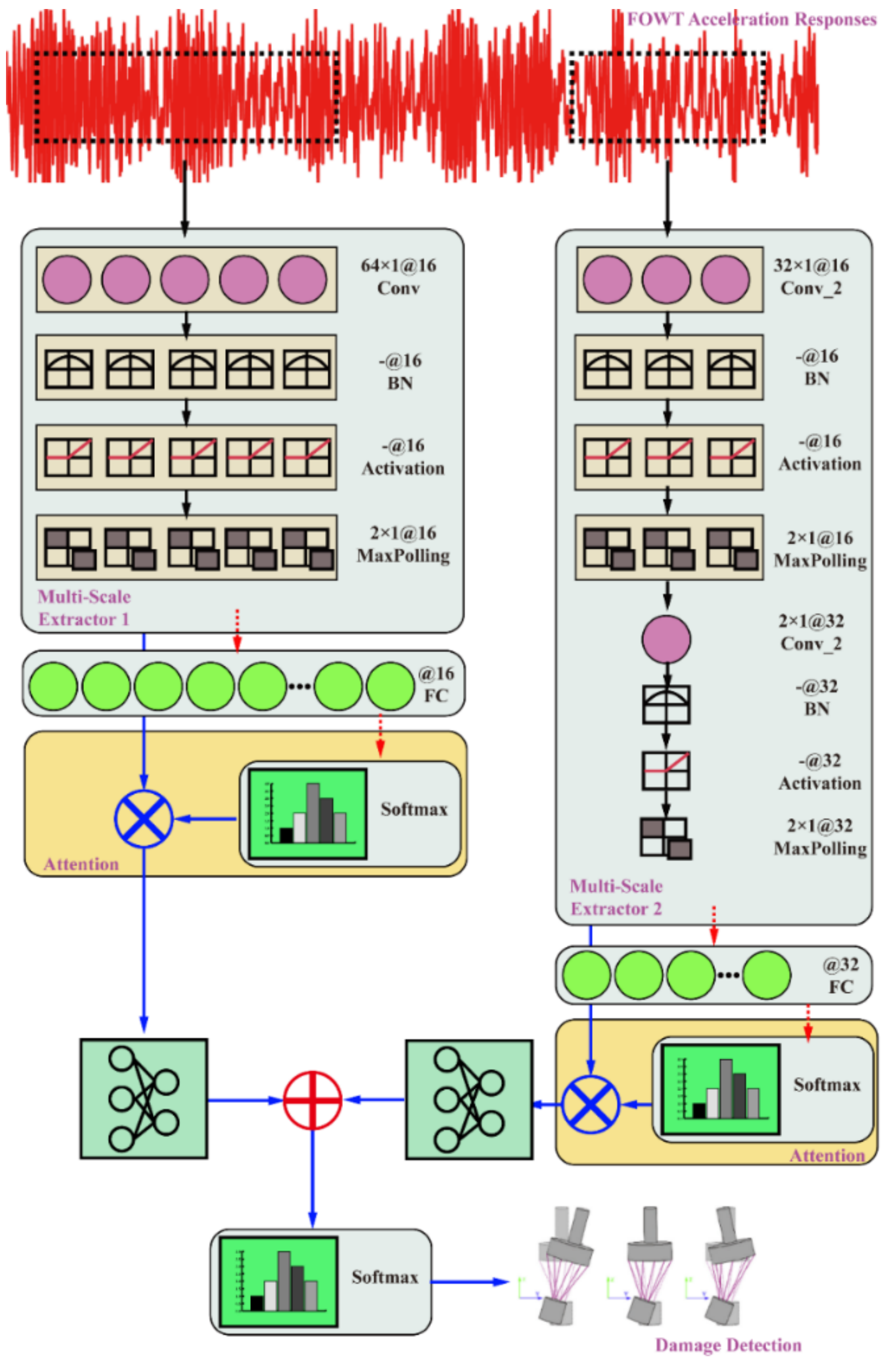

Figure 4: The architecture of MS-ACNN model for tendon damage detection

As shown in Figure 4, raw response signals of the FOWT are used as the input in the MS-ACNN model. The model is fitted with two parallel multi-scale extractors, which act on the raw signals to capture multi-scale features. The operating principle of the filters is that it is fitted with different kernel size, which has a better capability in extracting multi-scale information from a signal. Consequently, a multi-scale extractor with different depths of a network would have capability in obtaining different advanced features. The attention mechanism is used to give weights to every channel feature so that its contribution in probability calculation can be adequately evaluated. The values of the two parallel extractors are first added and then calculated by the Softmax function to obtain the pattern probabilities of FOWT tendon damage. The MS-ACNN model is optimized by the Adam gradient descent [31], in which the loss is defined as cross entropy for the purpose of realizing the tendon damage localization [32]. It should be noted that another purpose of using the Adam gradient descent is to optimize the MS-ACNN parameters, where the loss is treated as the root mean square to realize damage magnitude recognition [33].

3.2 MS-ACNN network with Majority Weighted Voting for multisensory collaborative diagnosis

The MS-ACNN algorithm is an "end-to-end" model adopted to systematically extract multi-scale features from raw signals of FOWT and achieve a high-accuracy diagnosis performance without any manual intervention. The MS-ACNN models are trained using different sensors' signals. A Majority Weighted Voting (MWV) method based on PSO is used to fuse the diagnosis from each MS-ACNN model in order to improve the robustness of the overall performance of FOWT's PHM method. The robustness of the MS-ACNN acts as a foundation for the multisensory collaborative diagnosis needed for predictive maintenance of FOWT. The framework of the MS-ACNN network fitted with MWV is presented in Figure 5.

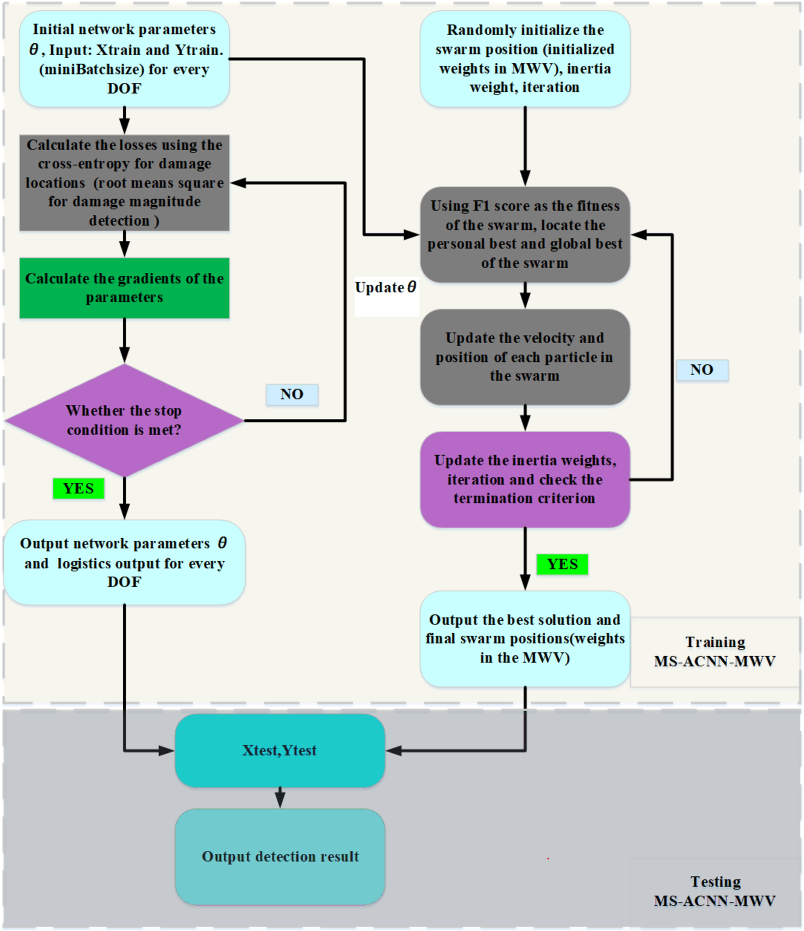

(a) The flowchart of the proposed MS-ACNN-MWV

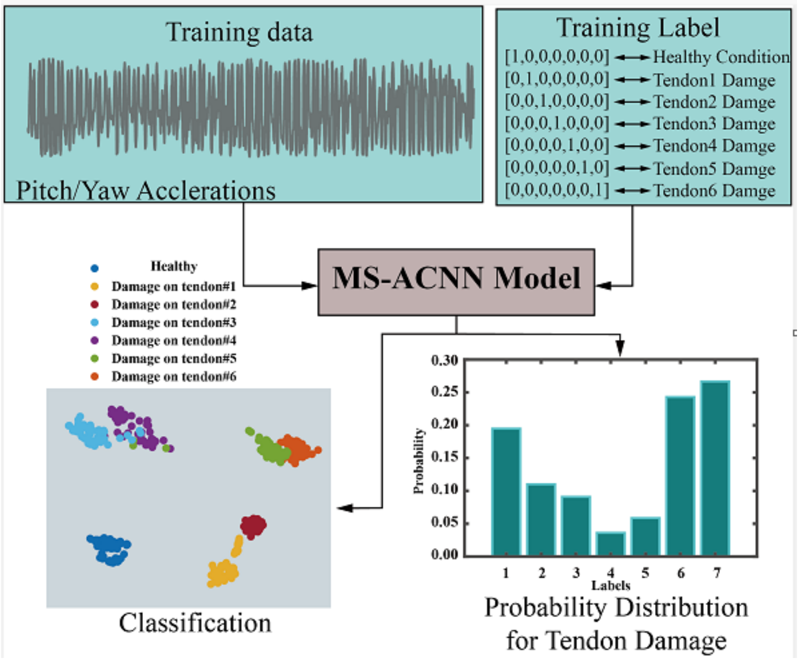

(b) The input and output of the MS-ACNN model

Figure 5: The flowchart of the proposed MS-ACNN-MWV for FOWT fault detection

The operating principle of the MS-ACNN network framework is as follows. First, data from different sensors with different DOFs is used to train the MS-ACNN networks. This is followed by incorporation of the PSO algorithm to solve the voting weight of each MS-ACNN's recognition of the FOWT state, leading to the design of the framework as MS-ACNN-MWV model. The state of FOWT tendons' health is established by using the collected data to be tested in the trained MS-ACNN-MWV model.

The MWV module treats each damage prediction as the final class label in which the choice of feature weights directly affects the final result of the diagnosis. Details of mathematical representation of the MWV within the framework are shown in Equation 10.

$$\mathrm{H}(x) = C_{arm\,\mathrm{ax}_j} \sum_{n=1}^{N} w_n h_n^j(x) \tag{10}$$

where $h_n^j(x)$ is the predicted nth sub-model for each probability (x). w_n is the weighted majority voting for each of the predicted nth sub-model ($h_n^j(x)$). The final predicted damage label, $\mathrm{H}(x)$, is calculated by using the $C_{arm\,\mathrm{ax}_j}(\cdot)$ function to determine the prediction that has the most votes.

Based on the conventional knowledge that the weighted majority voting rule depends on weights, this study uses a PSO [34], [35] to predict the optimized weights for application in the majority voting. The motivation for adopting this approach (using the PSO method) is to evaluate weights and facilitate the improvement of the F1 score of the MS-ACNN framework for multisensory collaboration [36]. The F1 score is a critical component used in determining the fitness functions of the PSO. The weights in the MWV are $w_n^c = [w_n^1, w_n^2, \ldots, w_n^c]^{\mathrm{T}}$ and they are based on the assumption that the MS-ACNN model is capable of solving the c-classification problem within the framework.

4. Detection Framework and MS-ACNN-MWV Flowchart

4.1 Data collection

The acceleration signal from 6 DOF of the floating body is collected at a sampling frequency of 10 Hz for use in this study. The collected data includes samples from different damage locations and damage magnitudes. Note that the damage induced in the tendon is based on reduction in magnitude of stiffness from of 5% to 50%.

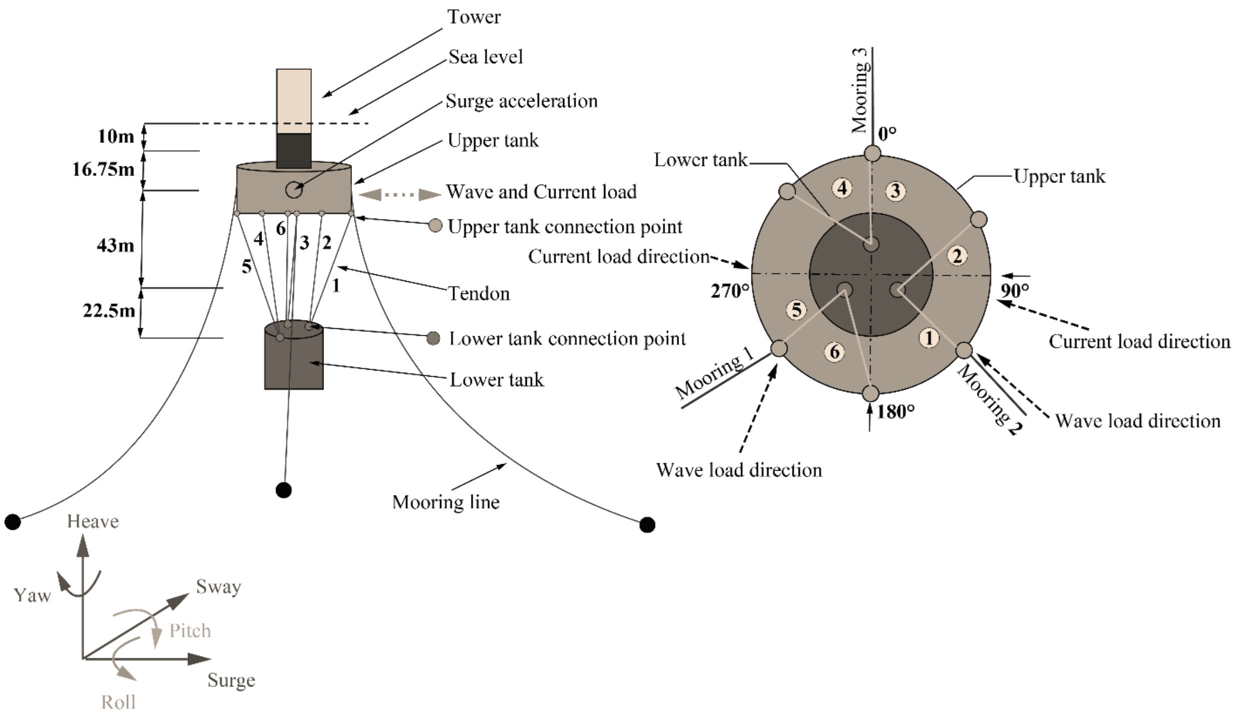

Figure 6: Schematic of tendon configurations in a multibody FOWT platform

4.2 Data normalization & samples segmentation

In order to obtain unbiased data for training the MS-ACNN network, data normalization, as part of preprocessing of the data, is conducted. The FOWT data is predicted from tendons (Figure 6) using different sensors, hence the collected data consists of response data for different degrees of freedom, including features such as speed, acceleration, and displacement. The data contains different features, and this requires normalization in order to provide a reliable diagnosis. In this study, the datasets are normalized using *z-score* normalization in which both mean standard deviation are zero. The method is commonly used as a data normalization technique [37].

In the training phase only, the datasets are further pre-processed based on an augmented sampling technique in which data-points are overlapped to augment the training data. However, the technique was not applied to the test samples because the tests data in the testing phase is independent.

Detailed information about the training/validation/testing dataset is shown in Table 2.

Table 2: Datasets of tendon damage of FOWT for multiple tasks

Datasets	Samples	Number of samples	Used Parameters
Damage Location Detection	Training	200	Pitch acceleration Yaw acceleration
	Validation	50	
	Test	100 (50 for multisensory)	
Damage Degree Recognition	Training	200	Pitch acceleration Yaw acceleration
	Validation	50	
	Test	100 (50 for multisensory)	

4.3 The MS-ACNN network's hyper-parameters setting and F1 estimators

The hyper-parameter settings of the neural network have a certain impact on the network performance. In order to overcome this impact, a dropout technique is used before the fully connected layer in the neural network with a dropout rate of 0.5 [38]. The neural network has an initial learning rate of 0.001 and fitted with the Adam optimization method [30]. An assessment of the impact of this addition has been investigated by comparing the performance of the MS-ACNN model integrated with hyper-parameters with other NN models such as MSCNN-I [28], MSCNN-II [29], CNN, CNN-LSTM and CNN-Bi-LSTM whose parameters are similar to the hyper-parameters.

In order to guarantee and sustain the model's accuracy during feature learning and classification phases, F1 score is used in comparison and evaluation of the diagnosis model's performance in this study. F1's mathematical definition is presented in Equation 11.

$$\mathrm{F1}=\frac{2\mathrm{TP}}{2\mathrm{TP}+\mathrm{FP}+\mathrm{FN}} \tag{11}$$

where TP, FP, TN and FN respectively represent faults correctly classified as positive samples, wrongly classified faults as positive samples, faults correctly classified as negative and wrongly classified faults as negative respectively.

5. Discussion and Results

In this section, the reliability of the developed MS-ACNN-based SHM method is examined using a dataset that includes 5% potential structural damage (minor faults) occurring at a location on different tendons of the FOWT. The first step in the examination is the use of responses from different DOFs collected as acceleration to train the MS-ACNN model to search the most useful characteristics for fault locations.

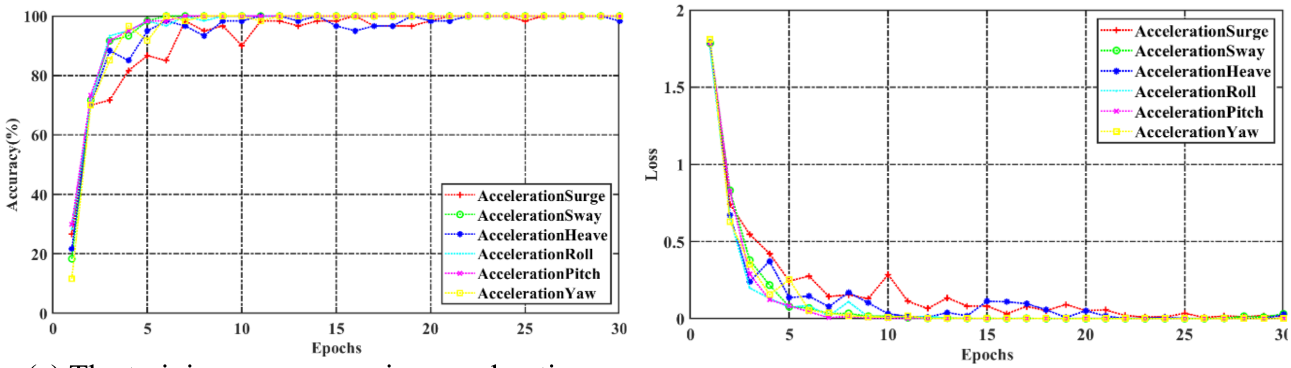

(a) The training accuracy using acceleration dataset to train the model

(b) The training loss using acceleration dataset to train the model

Figure 7: Training information under different DOFs to train MS-ACNN model

From the results presented in Figure 7, it is observed that training the MS-ACNN model with pitch and yaw responses as the feature dataset is much easier than using the responses from sway, roll, surge and heave. A corollary to this observation is that when the sea conditions change, the heave and pitch are the most sensitive because the wind-wave loads act perpendicularly on the wind rotor in the same direction. Therefore, in the subsequent validation of the MS-ACNN-based SHM method, acceleration responses acting along the pitch and yaw axes are used as dataset for training and testing.

5.1 Comparison of anti-noise examination of diagnosis methods

The procedure of FOWT response signal acquisition is often characterized by noise interference. Therefore, the robustness of a PHM method in noisy scenarios is particularly important. Dataset for the 50% structural damage condition was used as the training samples for all the training models, including CNN, MSCNN-I, MSCNN-II, CNN-LSTM, CNN-Bi-LSTM, and the proposed MS-ACNN.

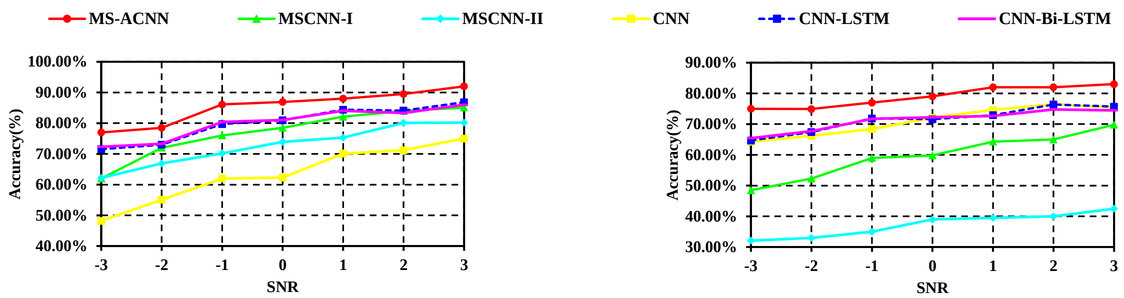

(a) Anti-noise assessment by Pitch (b) Anti-noise assessment by Yaw

Figure 8: Comparison of anti-noise assessments for diagnosis methods.

As shown in Figure 8, the MS-ACNN model has a superior diagnostic accuracy of nearly 80% in a large-noise testing background compared to other algorithms. Although the application of MSCNN models including MSCNN-I and MSCNN-II has demonstrated good performance in wind turbine gearbox faults diagnosis, the models do not perform as good as the deep convolutional networks in the diagnosis of FOWT tendons damage. This is because the response cycle of the FOWT is much slower than the gearbox, causing the deeper features in a neural network to have a negative effect in the classification task. This proves the superiority of using the proposed MS-ACNN model in the damage detection of FOWT tendons than most of the current industrial grade CNN models in use. In consideration of the long-term dependencies of the responses of FOWT, the results show the capability of fault recognition of the proposed MS-ACNN model in comparison to respectively using LSTM and Bi-LSTM combined with CNN. The proposed model fitted with multi-scale resolution with an attention mechanism offers better performance than other models that consider long-term dependencies. Furthermore, to explain the performance of convolution network features using the analogy of a black box, the key features in the multi-scale filters and advanced features are shown and visualized via t-distributed stochastic neighbor embedding (T-SNE) in the next section.

5.2 Features visualization

In order to explain what features the proposed MS-ACNN model has learned from the responses when the datasets with a damage magnitude of 15% is used, the acceleration responses of pitch and yaw in the different depth of the MS-ACNN model are presented as time series in Figure 9. Furthermore, Figure 9 also presents the features extracted by the MS-ACNN model and the network's structure of different scales (every channel's features).

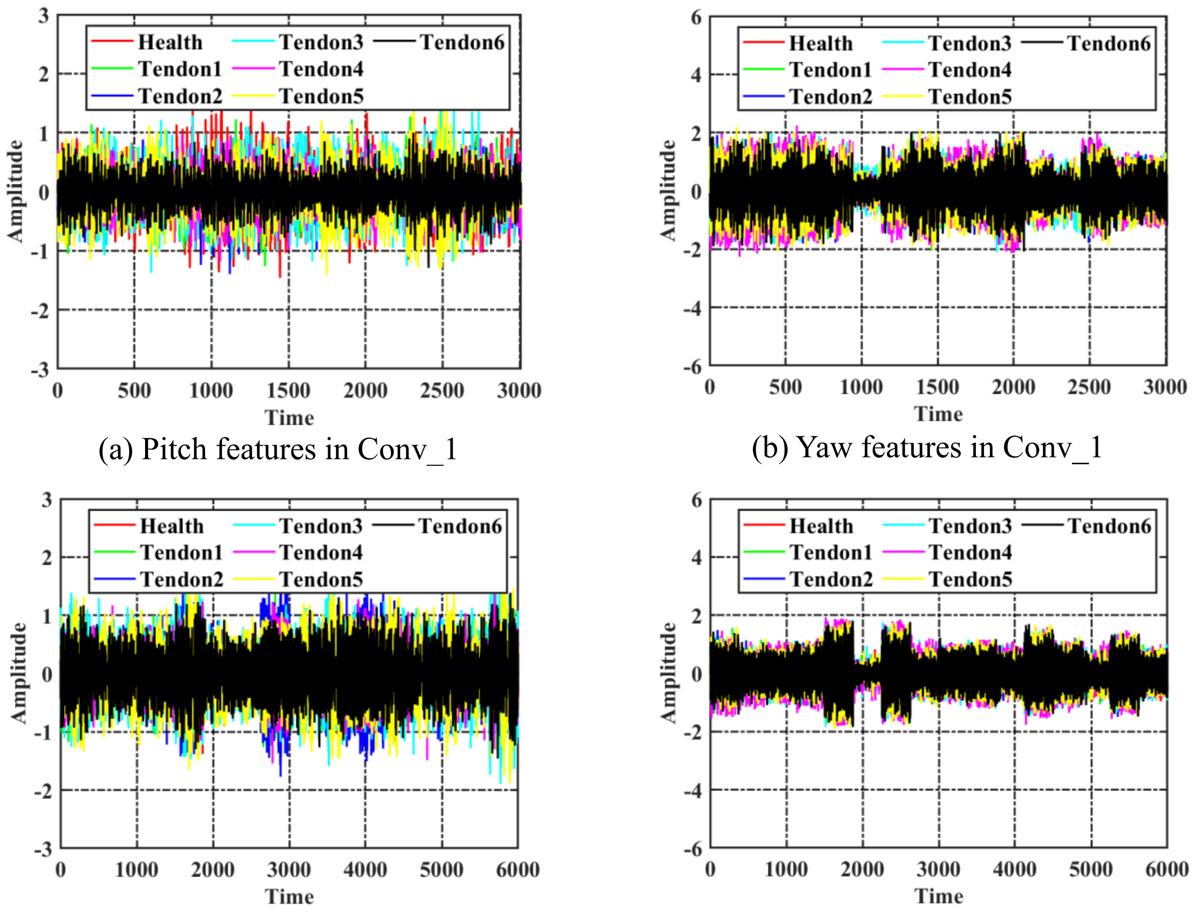

(a) Pitch features in Conv_1

(b) Yaw features in Conv_1

(c) Pitch features in Conv_2

(d) Yaw features in Conv_2

Figure 9: The time series of the features in multi-scale Convolution modules with 15% FOWT tendon damage.

As shown in Figure 9, Conv_1 and Conv_2 are filters with different convolution kernel sizes. The features in Conv_1 and Conv_2 have different scales of information. It is observed that in the features filtered by Conv_2, the responses of tendon 6 are more significant than those of the other two filters. This indicates that the relatively small size of the convolution kernel can capture the response characteristics of a FOWT when tendon 6 has little damage. In order to further explain what features are filtered by the multi-scale convolution modules in the MS-ACNN, an attempt to visualize the advanced features of FOWT responses by T-SNE was made.

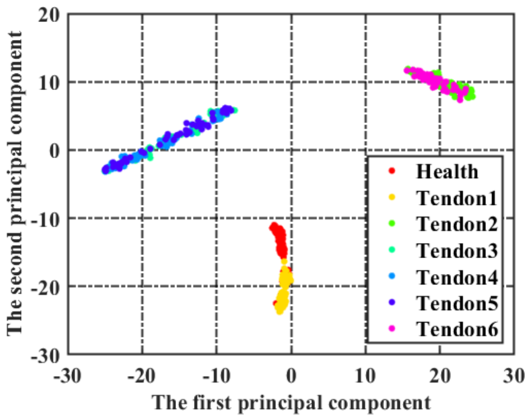

(a) Clustering of pitch from multi-scale 1

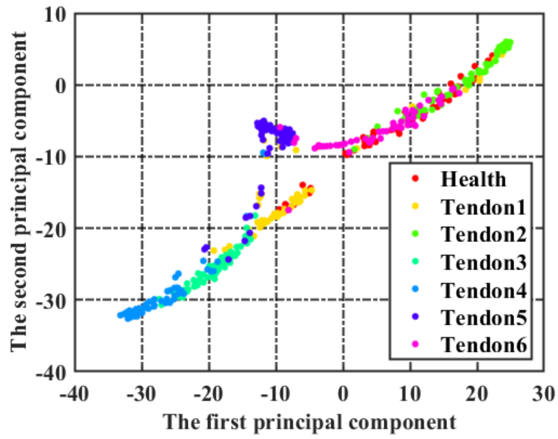

(b) Clustering of yaw from multi-scale 1

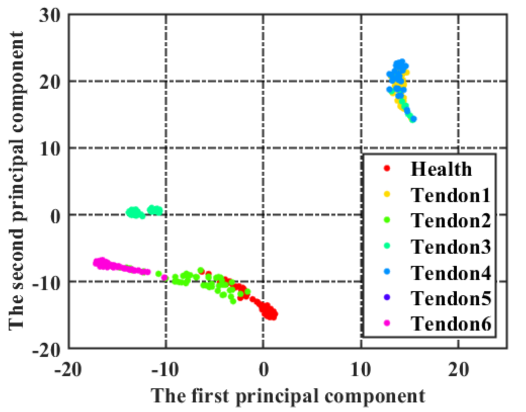

(c) Clustering of pitch from multi-scale 2

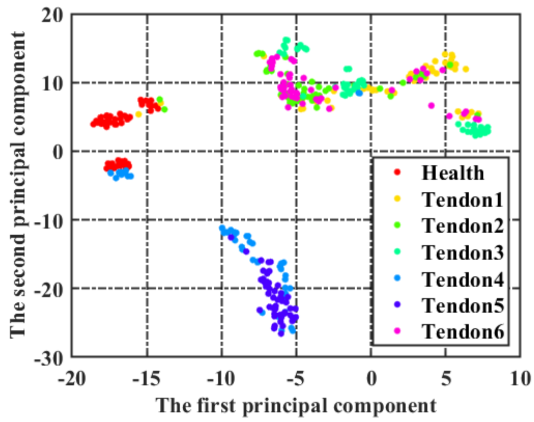

(d) Clustering of yaw from multi-scale 2

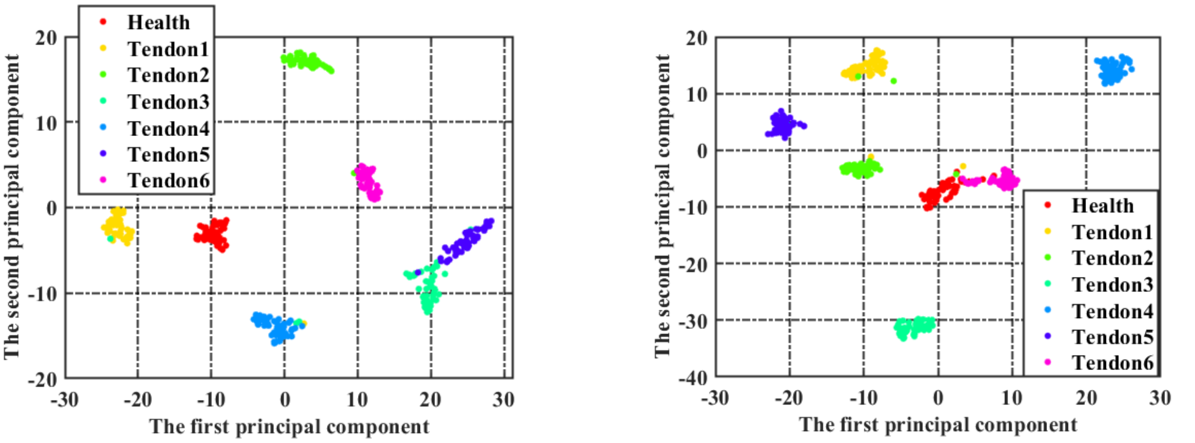

(e) Clustering of pitch from fusion features (f) Clustering of yaw from fusion features

Figure 10: The clustering results of the features in multi-scale Convolution modules for 15% FOWT tendon damage

Figure 10 (a-f) shows that the data points of 7 tendons states (including healthy state) are visualized from a two-dimensional plane through T-SNE. The clustering states of pitch and yaw have different effects in different scale feature-learning modules. Compared to Figures 10(b) and (d), and using a cluster of yaw as an example, the health state of FOWT tendons can be well distinguished from the tendons damage through the multi-scale module 2, but not through the multi-scale module 1. In Figure 10 (f), the fusion of outputs corresponding to the features in the multi-scale modules (to obtain the fused feature), demonstrates that the developed MS-ACNN can complement the advantages of the two scales learned from the FOWT responses for pattern recognition and offer a better classification performance.

To demonstrate the influence of wind-wave actions on the damage conditions during classification performance, the clustering results of the features in the fusion layer are presented in Figure 11.

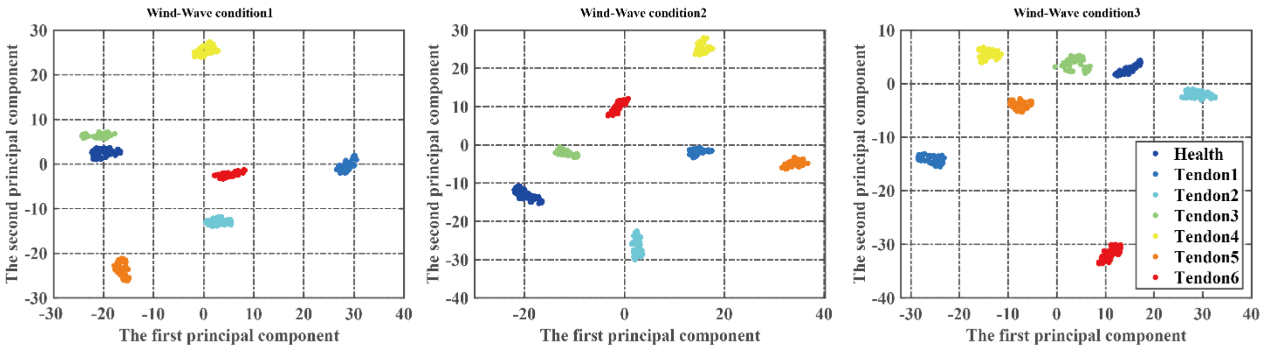

(a) Clustering of pitch from fusion features

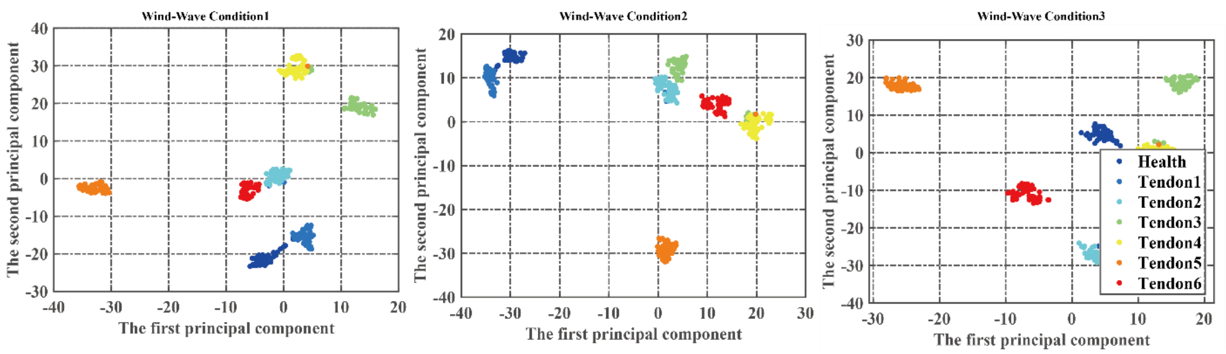

(b) Clustering of yaw from fusion features

Figure 11: The clustering results of features in multi-scale Convolution modules for 30% FOWT tendon damage under different wind-wave conditions

As shown in Figure 11, the clustering results of the features in MS-ACNN model for 30% tendon damage are all distinguished by t-SNE compared with the clustering results in Figure 10. This is significant in interpretation of the clustering results since a much larger damage magnitude will bring more significant responses. In comparison with the diagnosis results of pitch and yaw, the classification performance based on pitch response is still clearer than those from yaw. The clustering results of the multi-scale fused features in the MS-ACNN model show different clustering forms due to changes in the wind-wave condition. In Figure 11(b), the distance between the clustering points of different tendon damages changes with the wind-wave condition.

5.3 Detection of damage location

To further prove the robustness and superiority of the newly developed diagnostic module (MS-ACNN) for the PHM method, the performance of MS-ACNN in locating damage on tendons was examined. Damage tests with magnitudes ranging from 5% to 45% are used to examine the MS-ACNN model. The test result is presented in a confusion matrix.

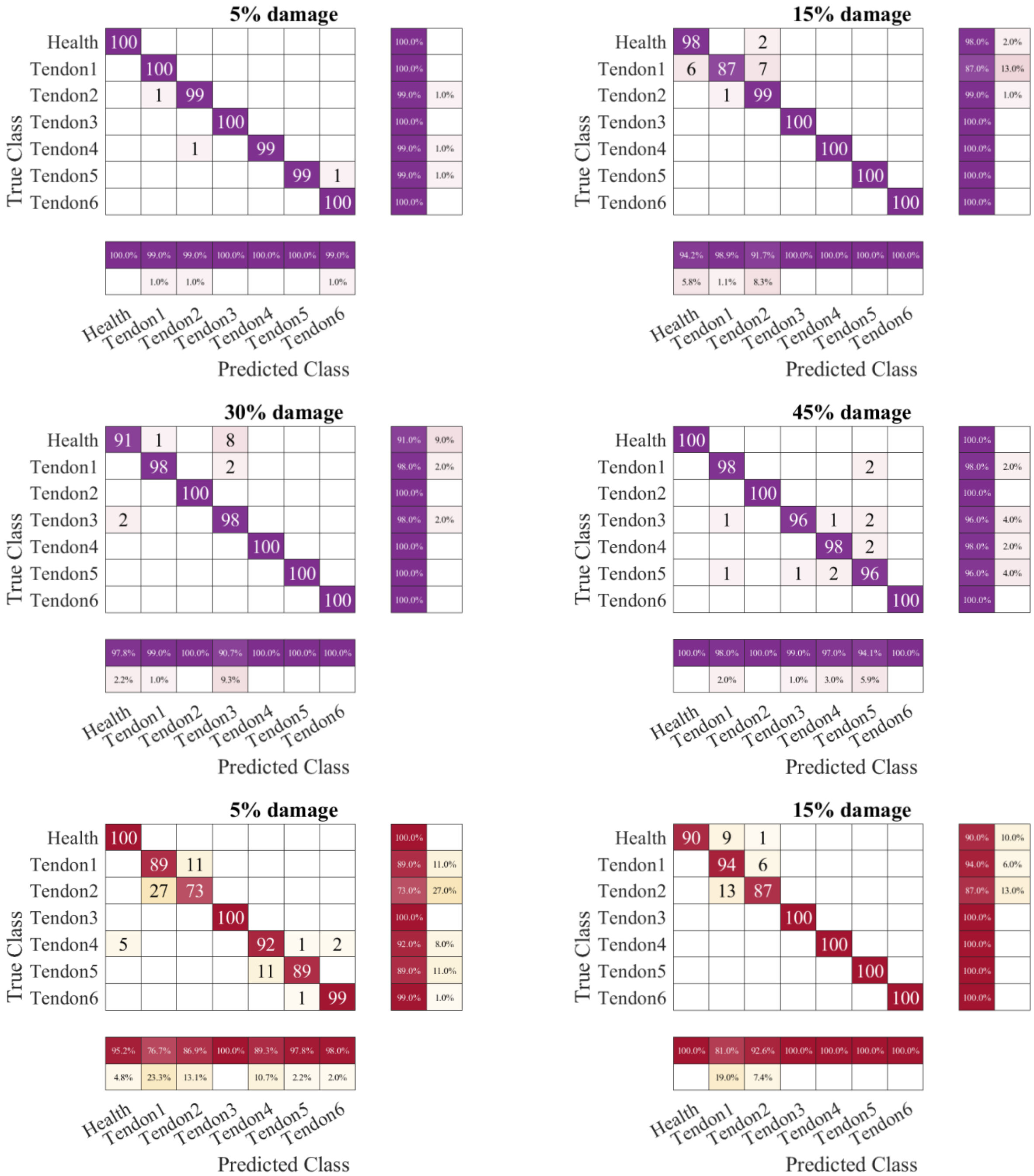

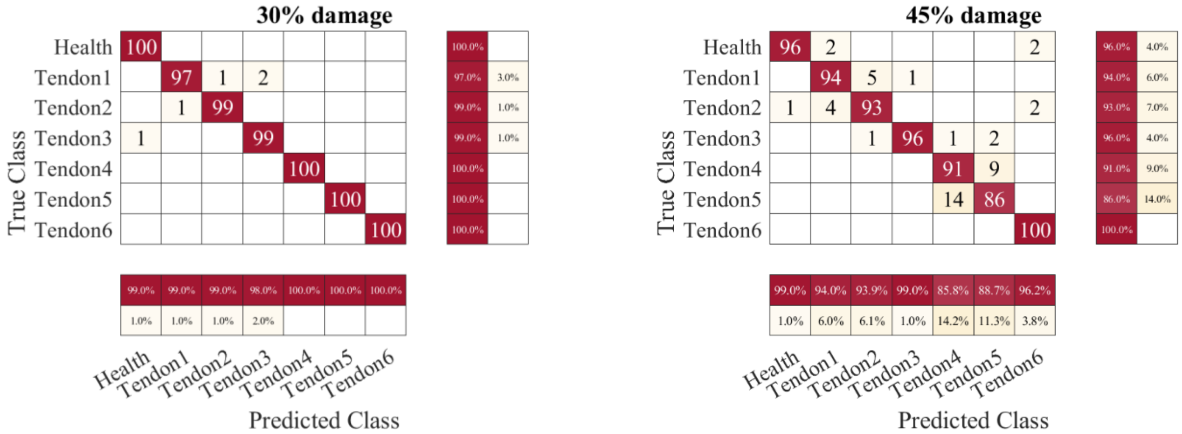

Figure 12: Performance of MS-ACNN model in detecting damage locations

As shown in Figure 12, the MS-ACNN model trained using the pitch and yaw responses has different degrees of sensitivities in identifying the damaged tendon. The pitch response is more sensitive to weak (lower stiffness [5% - 25%]) structural damage. Therefore, the MS-ACNN model trained by the pitch responses has a lower false alarm rate than the model trained by the yaw responses. However, when the structural damage increases to 30%, the model trained based on the yaw responses has a better diagnostic performance than the model trained by the pitch responses. In addition, when the structural damage increases to 45%, the models trained by both pitch and yaw responses have different false alarms for different damage locations. The pitch-response trained model usually has a false alarm in tendons 3, 4 and 5. On the other hand, the yaw-response trained model has a false alarm in the normal state and tendons 1 and 2 damages. Again, this is a clear demonstration of the significance of using multi-sensor collaboration to achieve accurate FOWT tendons damage diagnosis for PHM.

5.4 Damage magnitude detection

In order to examine the MS-ACNN model's extrapolation capability of damage magnitude detection as part of the model's intelligence, training datasets with damage magnitudes of 5%, 10%, 15%, 20% and 25% are used. Equally, the corresponding testing datasets used are for damage rates of 10%, 15%, 20%, 25% and 30%. As an example, the MS-ACNN model trained by 5% damage dataset was compared with a random test result (e.g.10% damage dataset test result) to assess the accuracy of its predictive performance. The results are presented in Figure 13.

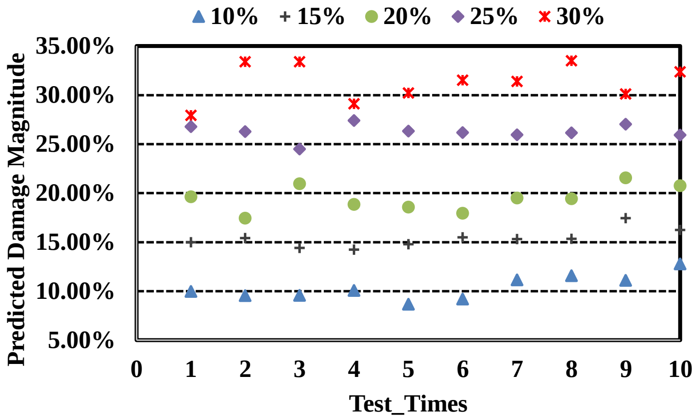

(a) The magnitute detection tested by pitch response for tendon#6

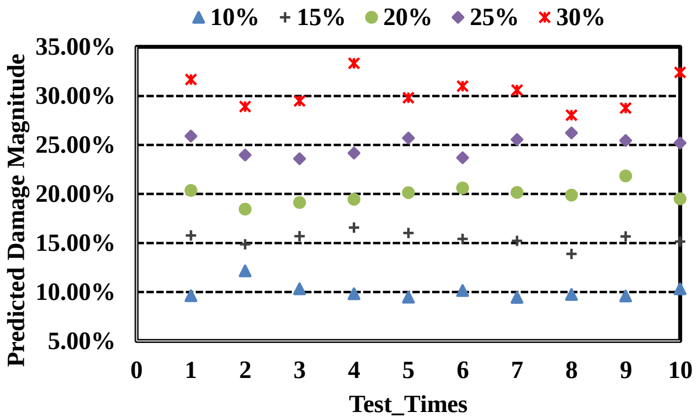

(b) The magnitute detection tested by yaw response for tendon#6

Figure 13: Damage magnitude detection for tendon 4 and tendon 6 by the MS-ACNN model

It is shown in Figure 13 that the MS-ACNN model recognizes the magnitude of small damage of tendon 6 better than the detection for a larger damage magnitude. For identification of a small damage magnitude in tendon 6, which has an inconsistent data distribution for both training and testing datasets, it is still observed that the MS-ACNN model offers a good regression performance in detecting the damage. This further reassures that the MS-ACNN model has good robustness in the identification of damage magnitude.

5.5 Multisensory collaborative diagnosis

Previous studies have shown that using response-based features with different DOFs to train MS-ACNN models can be complicated, especially if each MS-ACNN model has a different level of accuracy for tendon damage diagnosis. Therefore, in this section, a MWV method that uses a PSO algorithm [38] to fuse diagnosis results from the MS-ACNN models in the decision-making level is introduced.

The potential damage datasets of tendons damage with 50% are used to verify the reliability of the proposed decision fusion. The results of this examination prove the feasibility of adding MWV into the PHM method to form a new MS-ACNN-MWV approach for intelligent FOWT tendons diagnosis. It should be noted that in order to reflect the robustness of MS-ACNN-MWV in the developed framework, the MS-ACNN model is trained with 45% damage dataset, while the test data from 50% damage dataset is used.

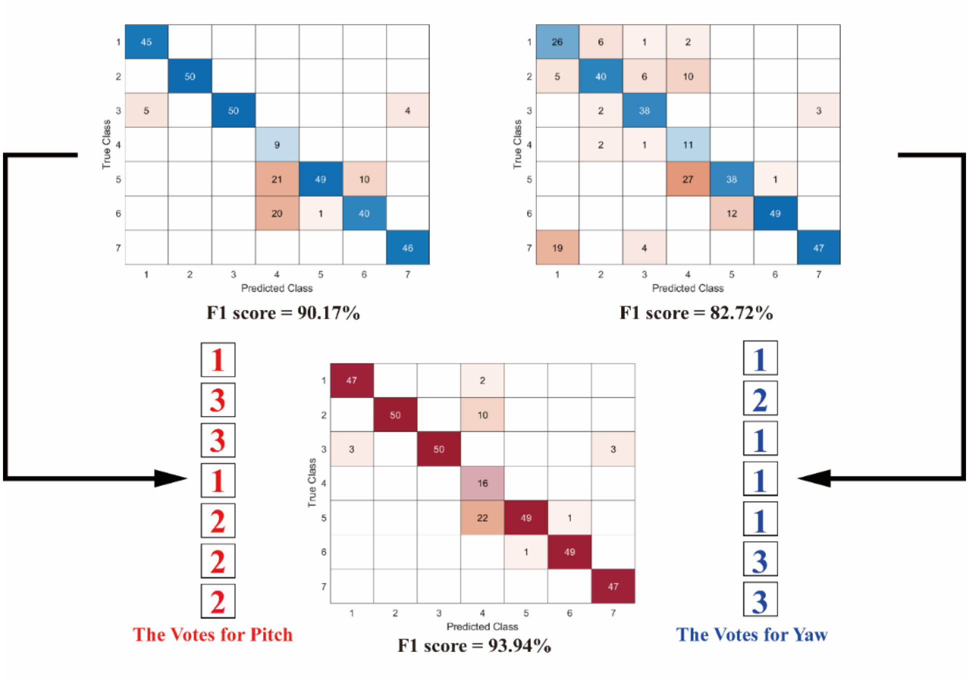

Figure 14: Confusion matrix of the MS-ACNN-MWV method

From Figure 14, it can be seen that MWV gives different weights to the decisions in the MS-ACNN models from pitch and yaw responses, which yields an average F1 score of 93.94%. Although the training and test datasets are derived from different damage magnitude data, the MS-ACNN model shows a good generalization capability, for pitch and yaw with nearly 90% and 83% F1 averages, respectively. The decision from the MS-ACNN model of yaw responses offers a better performance than the one of pitch responses when diagnosing tendon 5 and tendon 6 damages. Thus, the MWV gives more votes to the yaw MS-ACNN model decision than for pitch. The decision from the MS-ACNN model for pitch offers better performance than the decision for yaw when diagnosing healthy conditions, tendon 1 and tendon 2 damages. Thus, the MWV model gives more votes to the pitch MS-ACNN model decision than yaw for health states. In summary, it has been demonstrated that the MWV model can significantly reduce the false positive rate in the diagnosis. This also proves the industrial (engineering) applicability of MS-ACNN-MWV in the PHM method based on its good performance.

6. Conclusions

This research developed an end-to-end multi-sensor collaborative damage recognition method based on deep learning technique to support structural health monitoring of a 10MW FOWT's tendons as part of PHM. A novel multi-scale convolution neural network framework has been developed in this study. The framework contains multiple multi-scale feature extractors that can directly capture damage or faults features at different levels using the FOWT response signals. An attention mechanism is added to the framework to assign advanced feature weights in order to ensure that each channel feature has the best contribution in calculating the probability of damage occurrence for predictive diagnosis.

This investigation uses the structural damages of the 10MW FOWT tendons as a basic scenario to establish a dataset from multisensory sources for different damage locations and magnitudes from different DOFs on the tendon. The study found that using pitch and yaw acceleration signals offer an easier means to train the MS-ACNN model than the other four degrees of freedom signals. Two MS-ACNN models are trained with yaw and pitch acceleration signals respectively, and they have an 80%

diagnostic accuracy in a large noise background. In comparison to the existing multi-scale models used in the industry, MS-ACNN offers better performance that is at least 15% higher than most of the existing models do. Although performance tests reveal that the MS-ACNN model can offer different levels of superiorities when using either pitch and yaw acceleration signals, the accuracy of damage detection for smaller magnitudes of damages, usually the most difficult in practical applications, has been excellent as demonstrated by the study on tendon damages between 5% and 30%. In addition, the MS-ACNN model can also identify tendons with different damage magnitudes, when the tendons of a FOWT have weak stiffness changes. The addition of a proposed MWV method into the MS-ACNN module for diagnosis provided results, based on fusion of different sensors, that can improve the diagnosis performance by at least 4%.

Acknowledgements

This project is funded by European Regional Development Fund (ERDF), Interreg Atlantic Area (grant number: EAPA_344/2016) and the European Union's Horizon 2020 research and innovation programme under the Marie Skłodowska-Curie grant agreement no. 730888 (RESET).

References

[1] Yang, Yang, Musa Bashir, Jin Wang, Constantine Michailides, Sean Loughney, Milad Armin, Sergio Hernández, Joaquín Urbano, and Chun Li. "Wind-wave coupling effects on the fatigue damage of tendons for a 10 MW multi-body floating wind turbine." Ocean Engineering 217 (2020): 107909.

[2] Dinwoodie I, and McMillan D. (2014). Operation and maintenance of offshore wind farms. Engineering Technology Reference. ISSN 2056-4007.

[3] Zhao X-G. and Ren L-Z. (2015). Focus on the development of offshore wind power in China: has the golden period come? Renewable Energy 2015;81:644–57.

[4] Stehly T. J, and Beiter P. C. (2018). Cost of wind energy review. Technical report. Golden, CO (United States): National Renewable Energy Lab.(NREL); 2018. 2020

[5] Ren P, and Zhou Z. (2012). A state-of-the-art review on structural health monitoring of deepwater floating platform. Pacific Science Review;14(3):253–63.

[6] Jahangiri V, Mirab H, Fathi R, Ettefagh MM. (2016). TLP structural health monitoring based on vibration signal

of energy harvesting system. Latin American Journal of Solids and Structures 2016;13(5):897–915.

[7] Wang P, Tian X, Peng T, Luo Y. (2018). A review of the state-of-the-art developments in the field monitoring of offshore structures. Ocean Engineering;147:148–64.

[8] Shittu A.A, Mehmanparast A, Wang L, Salonitis K, Kolios A. (2020). Comparative study of structural reliability assessment methods for offshore wind turbine jacket support structures. Applied Science 2020, 10 (3), 860.

[9] Tahan M, Tsoutsanis E, Muhammad M, Abdul K.Z.A. (2017). Performance-based health monitoring, diagnostics and prognostics for condition-based maintenance of gas turbines: A review. Applied Energy 2017;198:122–44

[10] Li X, Liu J, Bai M, Li J, Li X, Yan P, Daren Y. (2021). An LSTM based method for stage performance degradation early warning with consideration of time-series information. Energy; vol 226(C), 120398.

[11] Tang S, Tang H, Chen M. (2019). Transfer-learning based gas path analysis method for gas turbines. Applied Thermal Engineering 2019;155:1–13

[12] Zhao Z, Wu J, Li T, Sun C, Yan R, Chen X. (2021). Challenges and Opportunities of AI Enabled Monitoring, Diagnosis & Prognosis: A Review. Chinese Journal of Mechanical Engineering;34(1):1–29.

[13] Liu P.L. and Sun S.C. (1997). The Application of Artificial Neural Networks on the Health Monitoring of Bridges. Structural Health Monitoring, Current Status and Perspectives, Stanford University, Palo Alto, California, 1997, pp. 103–110

[14] Nguyen C, Huynh T, Kim J. (2018). Vibration based damage detection in wind turbine towers using artificial neural networks, Structural Monitoring and Maintenance. 5 (4) (2018) 507–519

[15] Dervilis N, Choi M, Taylor S.G, Barthorpe R.J, Park G, Farrar C.R, Worden K, (2014). On damage diagnosis for a wind turbine blade using pattern recognition, Journal of Sound and Vibration. 333 (2014) 1833e1850.

[16] Avci, O., Abdeljaber, O., Kiranyaz, S., Hussein, M., Gabbouj, M., Inman, D. J. (2021). A review of vibration-based damage detection in civil structures: From traditional methods to Machine Learning and Deep Learning applications. Mechanical Systems and SignalPprocessing, 147, 107077.

[17] Gul, M., & Catbas, F. N. (2011). Damage assessment with ambient vibration data using a novel time series analysis methodology. Journal of Structural Engineering, 137(12), 1518-1526.

[18] Choe, D. E., Kim, H. C., & Kim, M. H. (2021). Sequence-based modeling of deep learning with LSTM and GRU networks for structural damage detection of floating offshore wind turbine blades. Renewable Energy, 174, 218-235.

[19] Xiang, L., Yang, X., Hu, A., Su, H., Wang, P. (2022). Condition monitoring and anomaly detection of wind turbine based on cascaded and bidirectional deep learning networks. Applied Energy, 305, 117925.

[20] Yang, X., Zhang, Y., Lv, W., Wang, D. (2021). Image recognition of wind turbine blade damage based on a deep learning model with transfer learning and an ensemble learning classifier. Renewable Energy, 163, 386-397.

[21] Azamfar, M., Singh, J., Bravo-Imaz, I., Lee, J. (2020). Multisensor data fusion for gearbox fault diagnosis using 2-D convolutional neural network and motor current signature analysis. Mechanical Systems and Signal Processing, 144, 106861.

[22] Pan, Y., Hong, R., Chen, J., Singh, J., Jia, X. (2019). Performance degradation assessment of a wind turbine

gearbox based on multi-sensor data fusion. Mechanism and Machine Theory, 137, 509-526.

[23] Pan, Y., Hong, R., Chen, J., Feng, J., Wu, W. (2021). Performance degradation assessment of wind turbine gearbox based on maximum mean discrepancy and multi-sensor transfer learning. Structural Health Monitoring, 20(1), 118-138.

[24] Abdulraheem, K. F., and Al-Kindi, G. (2018). Wind turbine condition monitoring using multi-sensor data system. International Journal of Renewable Energy Research (IJRER), 8(1), 15-25.

[25] Shao, H., Lin, J., Zhang, L., Galar, D., & Kumar, U. (2021). A novel approach of multisensory fusion to collaborative fault diagnosis in maintenance. Information Fusion, 74, 65-76.

[26] Yang Y, Bashir M, Li C, Wang J, (2021). "Investigation on mooring breakage effects of a 5 MW barge-type floating offshore wind turbine using F2A." Ocean Engineering (2021): 108887.

[27] Ifremer. Marine Data Portal, French Research Institute for the Exploitation of the Sea, Online: http://data.ifremer.fr/pdmi/portalssearch/main. Data Accessed: January 2019.

[28] Zhao, B., Zhang, X., Zhan, Z., Pang, S. (2020). Deep multi-scale convolutional transfer learning network: A novel method for intelligent fault diagnosis of rolling bearings under variable working conditions and domains. Neurocomputing, 407, 24-38.

[29] Jiang, G., He, H., Yan, J., Xie, P.. (2018). Multiscale convolutional neural networks for fault diagnosis of wind turbine gearbox. IEEE Transactions on Industrial Electronics, 66(4), 3196-3207

[30] Xu, Z., Li, C., Yang, Y. (2021). Fault diagnosis of rolling bearings using an improved multi-scale convolutional neural network with feature attention mechanism. ISA transactions, 110, 379-393.

[31] Kingma, D. P., and Ba, J. (2014). Adam: A method for stochastic optimization. arXiv preprint arXiv:1412.6980.

[32] Xu, Z., Li, C., Yang, Y. (2020). Fault diagnosis of rolling bearing of wind turbines based on the variational mode decomposition and deep convolutional neural networks. Applied Soft Computing, 95, 106515.

[33] Willmott, C. J., and Matsuura, K. (2005). Advantages of the mean absolute error (MAE) over the root mean square error (RMSE) in assessing average model performance. Climate research, 30(1), 79-82.

[34] Zi-Fei, X., Min-Nan, Y., Chun, L. (2019). Application of the proposed optimized recursive variational mode decomposition in nonlinear decomposition. ACTA PHYSICA SINICA, 68(23).

[35] Trelea, I. C. (2003). The particle swarm optimization algorithm: convergence analysis and parameter selection. Information processing letters, 85(6), 317-325.

[36] Xu, Z., Mei, X., Wang, X., Yue, M., Jin, J., Yang, Y., Li, C. (2021). Fault diagnosis of wind turbine bearing using a multi-scale convolutional neural network with bidirectional long short term memory and weighted majority voting for multi-sensors. Renewable Energy.

[37] Cheadle, C., Vawter, M. P., Freed, W. J., Becker, K. G. (2003). Analysis of microarray data using Z score transformation. The Journal of molecular diagnostics, 5(2), 73-81.

[38] Srivastava, N., Hinton, G., Krizhevsky, A., Sutskever, I., Salakhutdinov, R. (2014). Dropout: a simple way to prevent neural networks from overfitting. The journal of machine learning research, 15(1), 1929-1958.